Water Dynamics in Hardened Ordinary Portland Cement Paste or Concrete: From Quasielastic Neutron Scattering

Heloisa N. Bordallo,*,† Laurence P. Aldridge,‡ and Arnaud Desmedt§

Hahn-Meitner-Institut, SF6 Glienicker Strasse, 100, D-14109 Berlin, Germany, Senior Fellow Materials & Engineering Science ANSTO Australia & A/Prof School of Civil and Environmental Engineering, UNSW2234, Australia, and LPCM UMR5803 CNRS, Université de Bordeaux I, F-33405 Talence, Cédex, France

Received: May 12, 2006; In Final Form: June 22, 2006

Portland cement reacts with water to form an amorphous paste through a chemical reaction called hydration. In concrete the formation of pastes causes the mix to harden and gain strength to form a rock-like mass. Within this process lies the key to a remarkable peculiarity of concrete: it is plastic and soft when newly mixed, strong and durable when hardened. These qualities explain why one material, concrete, can build skyscrapers, bridges, sidewalks and superhighways, houses, and dams. The character of the concrete is determined by the quality of the paste. Creep and shrinkage of concrete specimens occur during the loss and gain of water from cement paste. To better understand the role of water in mature concrete, a series of quasielastic neutron scattering (QENS) experiments were carried out on cement pastes with water/cement ratio varying between 0.32 and 0.6. The samples were cured for about 28 days in sealed containers so that the initial water content would not change. These experiments were carried out with an actual sample of Portland cement rather than with the components of cement studied by other workers. The QENS spectra differentiated between three different water interactions: water that was chemically bound into the cement paste, the physically bound or "glassy water" that interacted with the surface of the gel pores in the paste, and unbound water molecules that are confined within the larger capillary pores of cement paste. The dynamics of the "glassy" and "unboud" water in an extended time scale, from a hundred picoseconds to a few nanoseconds, could be clearly differentiated from the data. While the observed motions on the picosecond time scale are mainly stochastic reorientations of the water molecules, the dynamics observed on the nanosecond range can be attributed to long-range diffusion. Diffusive motion was characterized by diffusion constants in the range of (0.6−2) 10^{-9} m^2/s, with significant reduction compared to the rate of diffusion for bulk water. This reduction of the water diffusion is discussed in terms of the interaction of the water with the calcium silicate gel and the ions present in the pore water.

Introduction

Microscopic motions involved in the diffusion of hydrogen-containing molecules can be very effectively studied by quasielastic neutron scattering (QENS). In fact, in the case of water this potential has been exploited for many years.[1] On the other hand, the behavior of water in confined geometries and near solid surfaces is relevant to many important processes ranging from industrial applications (catalysis and soil chemistry) to biological processes (protein folding or ionic transport in membranes). In the particular case of water in hydrating cement paste, it is widely accepted that the state of water influences its mechanical and transport properties, as well as directly impacts the durability of concrete structures.[2,3] As a consequence understanding the water behavior in cement pastes is essential from both scientific and technological views.

Mindess et al.[2] and Neville[3] review the hydration reaction from the perspective of both the chemistry and the microstructure of the hardened cement paste. The calcium silicates react with water to form the calcium silicate gel (defined as C−S−H) and calcium hydroxide. The stoichiometry of the reaction may vary according to the composition of the cement. If Ordinary Portland Cement (OPC) is used then the C−S−H has a Ca/Si molar ratio of about 1.8. Alternatively when the cement is blended with an active silica additive, such as Ground Granulated Blast Furnace Slag (GGBFS), the blended cement will react with the calcium hydroxide and the C−S−H will have a more silica rich composition of about 1.5 Ca/Si. Although such pastes can have superior properties in resisting the permeability of water, they can also hydrate at significantly slower rates.

According to Mindess et al.[2] when mixing cement pastes with a water-to-cement ratio of 0.42 (defined by weight as w/c) most cements will completely hydrate at long hydration times. Pastes with less water will self-desiccate leaving an unreacted cement and empty capillary pores while pastes with more water will have (if there is no evaporation) unbound water remaining in the capillary pores in the pastes. As the cement reacts with the water it forms chemically bound water either in C−S−H or a calcium sulphate aluminate phase or calcium hydroxide. The remaining water will be in either capillary or gel pores. As the

* Address correspondence to this author. Phone: +49 (0)30 8062 2924. Fax: +49 (0)30 8062 2781. E-mail: bordallo@hmi.de.
† Hahn-Meitner-Institut.
‡ Senior Fellow Materials & Engineering Science ANSTO Australia & A/Prof School of Civil and Environmental Engineering.
§ Université de Bordeaux I.

10.1021/jp062922f CCC: $33.50
Published on Web 08/22/2006

reaction proceeds the pore space which was originally between the unhydrated grains is filled or partially filled with hydration products. The rate and extent of reaction can be calculated from the ratio of unbound water to bound water. Free (or unbound) water can be estimated by the weight loss when heating the paste at 105 °C until constant weight and chemically bound water from the further loss of weight when heating the paste to 1000 °C. In most cement systems the cement does not completely hydrate even after several years and it is common to find mobile water and unhydrated cement in hardened cement pastes. However, the concrete performance at 28 days is taken as the norm for compressive strengths. In any scenario it is expected that pore water will not have the same properties as pure bulk water simply because the pore water contains substantial amounts of Na^+ Ca^{2+}, K^+, and OH^- ions with a total concentration of up to 1 mol per L[2].

Furthermore, the microstructure of the cement pastes is dependent on the water-to-cement ratio, and the size of the pores in the paste varies with a large range of sizes.[2,3] Capillary pores, which have greater equivalent diameter than 100 Å, are responsible for the majority of water transport in hardened cement paste. The smaller gel pores, ranging in diameter from 100 to less than 5 Å, will preferentially hold the mobile water and may include interlayer water analogous to clays. The actual volumes of the gel pores, the capillary pores, the hydrated cement products, and the unhydrated cement can be calculated from the Powers−Brownyard model[2,3] by using both the w/c ratio and the extent of the reaction. It should be noted that such calculations only give approximations depending on the different assumptions made in the two texts.[2,3] In addition, the gel pores are considered to be about one-fourth the volume of the cement hydration products. Thus this relatively large volume is filled with water, and here we suppose that it is the interaction of this water in the gel pores with the microstructure of the cement paste that dominates the behavior of the QENS described in this paper.

However, it is clear that defining the pores in hardened cement paste (or concrete) is still a controversial issue. Recently the controversies surrounding the determination of pore volumes and surface areas by various techniques were carefully reviewed.[4] A major problem is that the surface areas of pores measured by water adsorption are significantly greater than those measured from liquid nitrogen. Besides the surface areas change depending on the drying procedures. It appears that on water removal the gel pores in the cement paste collapse; however, the collapse mechanism and indeed the interaction of the water with the gel pores is not yet understood. Another problem in comparing pores in pastes made from the same paste as starting materials but with different w/c ratios is that they hydrate at different rates. Thus pore volume at a specified time is related to the degree of hydration, not the w/c ratio.[4]

The interaction of the C−S−H and the water in the gel pores is critical to the understanding of many properties of cement paste. For example, it has been suggested that these properties control the shrinkage and the creep of concrete.[2,3] On the other hand, the capillary pores can dominate the transport of water in to and out of the cement paste simply because they are so much larger than the gel pores. Besides it has been shown that at pastes with w/c ratios of less than 0.4 the capillary pore exhibit discontinuities after short hydration times.[5] In this particular case it will be the gel pores that permit water to be transported in cement pastes.

Considering that QENS can give insight on the dynamics of confined or interfacial water[6−11] we have performed a series of QENS experiments to investigate the interaction of the water in the gel pores with the cement paste. Combining time-of-flight to backscattering techniques allowed observation on the dynamics of water in an extended time scale, from hundreds of ps to a few ns, on cement pastes made from commercial Portland cements and hydrated for more than 28 days. The results reveal that to a first approximation the QE response can be explained in terms of the diffusion of water within the gel pores within the paste. Our results show that QENS can be used to examine the interactions of the pore water to the pore structure in the paste.

TABLE 1: Details about the Hydration Level for Each Sample

instrument	sample name	w/c as prepared
NEAT	OPC-40°C	0.32[a]
NEAT	OPC-RT	0.42
NEAT	OPC-40°C	0.42
NEAT	OPC/GGBFS	0.42[b]
NEAT	OPC-40°C	0.6
HFBS	OPC-RT	0.4
HFBS	OPC-40°C	0.4

[a] Prepared with Reobuild 2000 Superplasticiser (based on water-soluble sulfonated polymers). [b] GGBFS ground granulated blast furnace slag (OPC:GGBFS 1:3 (by weight)).

Experimental Section

Samples were prepared from an Australian commercial cement made from the Berrima works. Water (40 g) was placed in a Wearing Blender stirrer, and the applicable amount of cement was added to make up the correct w/c ratio, then the mixture was stirred at low and then shear mixed at high speed for at least 60 s. The blended cement was made from mixing a commercial GGBFS obtained from the Port Kembla blast furnace mixed with the Berrima cement at a ratio of 1 OPC:3 GGBFS (by weight). Pastes with w/c less than 0.42 were prepared with additions of the superplasticizer Rheobuild 2000 to make the pastes flow. The pastes were cured for ∼28 days at either room temperature or 40 °C in a sealed plastic mould. Cement pastes, with different levels of hydration, as described in Table 1, were measured at room temperature (293 K). Crushed samples in the absence of CO_2 were confined between two Teflon sheets in a flat volume and sealed between aluminum disks in a glovebox flooded with helium. Time-of-flight (ToF) spectra were measured with the multichopper spectrometer NEAT,[12] located at the Hahn-Meitner Institut, using incident wavelengths of 8.1 or 5.1 Å, corresponding to elastic energy resolutions, ΔE, of 30 or 98 μeV (fwhm) within an angular range of $13.3° < \phi < 136.7°$. An orientation angle of $\alpha = 135°$ with respect to the incident neutron beam direction was used for all samples, including vanadium. When using this orientation the higher detectors have to be discarded. For the QENS data analysis, after removing Bragg peaks, the spectra were grouped to obtain nine constant angle spectra, resulting in a wave-vector transfer range of $0.25\ Å^{-1} < Q < 2.11\ Å^{-1}$. Furthermore, to analyze the short-time dynamics (inelastic response) of the water molecules we also obtained the generalized density of states (GDOS), within the framework of the "incoherent approximation".[13] As the transmission values vary between 0.88 and 0.84, it was not necessary to apply any multiple scattering corrections.

In addition, high-resolution QENS experiments were carried out at the National Institute of Technology (NIST) Center for Neutron Scattering Research with the HFBS spectrometer.[14] In this case a nominal wavelength $\lambda = 6.271$ Å gives an elastic energy resolutions ΔE of 1.1 μeV (fwhm) covering an angular

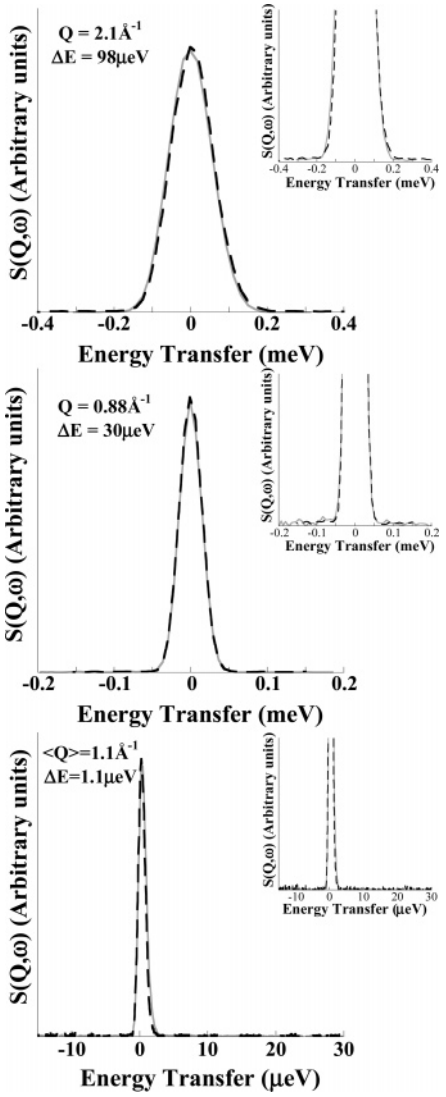

Figure 1. Typical spectra from a QENS experiment on dried cement pastes (line) and the resolution function (dashed line) at different *Q*-values. The original w/c ratio was 0.42 (OPC-RT). Upper panels: NEAT spectra recorded with $\Delta E = 98$ μeV. Middle panels: NEAT spectra recorded with $\Delta E = 30$ μeV. Lower panels: HFBS spectra recorded with $\Delta E = 1.1$ μeV. Notice that no broadening is observed within the resolution functions.

range of $14.46° < \phi < 121.25°$. To analyze the data each spectrum was averaged over the whole angular range covered by the spectrometer. This averaging procedure led to a better deconvolution of the QENS components, even if the *Q*-dependence of the protons dynamics cannot be analyzed.

In both experiments, after recording the QENS spectrum, each sample was dried at 105 °C in an oven to constant weight. The samples were then resealed and their spectrum was remeasured, under the same conditions, to determine the contribution coming from the chemically bound water. Figure 1 shows a comparison of the normalized spectra of the dried sample (w/c = 0.42) to that of the resolution function (vanadium spectra) at different *Q*-values. We can clearly observe that within the instrumental resolutions ($\Delta E = 1.1$, 30, or 98 μeV) no addition QE broadening was observed. In addition, it should be mentioned that the same observation has been done whatever the water-to-cement ratio was.

During the ToF experiment water was added to two cement pastes which had been dried at 105 °C. The samples chosen had the most and the least water (w/c = 0.32 and 0.60). They were placed inside a desiccator that contained water and the pressure was reduced. After about 12 h the pastes were weighted and the QENS spectra measured. As will be shown in the next section, the spectra were significantly different from those of the original paste.

Spectra correction, normalization, grouping, and transformation to the energy transfer scale were performed with the standard routines available at HMI and NIST.

Results

A. Short Time Dynamics. During the hydration process the free water will become either bound into C−S−H gellike structure or chemically react to form calcium hydroxide.[15,16] The short-time dynamics of the hydrogen atoms will mainly determine the inelastic part of the spectrum. Therefore, by using the incoherent one-phonon approximation, the *Q*-dependent density of states of the hydrogen atoms is given by:

$$G(Q,\omega) = \frac{M_{H_2O}}{k_B T}\left(\frac{\hbar\omega}{Q}\right)^2 \exp\left(-\frac{\hbar\omega}{k_B T}\right) S_H(Q,\omega) \qquad (1)$$

M denotes the mass of the scattering units (here the water molecule), k_B is the Boltzmann constant, T is the temperature, $h\omega$ gives the neutron energy transfer, and $S_H(Q,\omega)$ is the experimental incoherent scattering function (here dominated by the H-motion).

In Figure 2, we show the density of states in the range 0−120 meV averaged over all scattering angles ($\langle Q \rangle = 1.18$ Å^{-1}) for the samples with w/c = 0.42. To get a better understanding of our data, one has to consider two main points:

(i) Calculations of the quenched normal modes (QNM) in bulk water show a dip at about 44 meV separating two distinct groups of vibrations.[17] In particular, the low-frequency part ($0 < \omega < 44$ meV) is related to the translational degrees of freedom, whereas the higher frequency modes ($50 < \omega < 125$ meV) involve mostly rotational, indeed librational, degrees of freedom. This pronounced separation of the translational and rotational contributions to the QNM density of states undoubtedly has its origins in the difference between the overall (H, O) mass participating in the translation and the much lighter (H) mass defining the moments of inertia. Indeed measurements of the density of states of bulk water obtained by means of neutron and Raman scattering[18,19] confirm such a trend, with vibrational motions assigned as follows. The peaks around 6 and 20−35 meV correspond respectively to the bending of the O−O−O and to the stretching of the O−O units, while a broad vibration around 70 meV is related to librational modes. Furthermore, a mode observed at 33 meV at low temperatures and can be related to the 40 meV band seen in ice I, and most likely arises form differing electrostatic interactions in different configurations of coupled H bonds in neighboring H_2O molecules.

(ii) However, as in many processes, water does not exist in its bulk form, but in some sort of confined environment, with dynamics that are distinct from bulk water molecules. Thus in our particular case the vibrational spectra of the water molecules will also have a distinct *fingerprint* due to the fact that they are contained by the cement paste. We should then recall that for many years it has been accepted that such trapped water molecules may behave like supercooled water.[20] In this context water in confinement is seen as trapped in a cage formed by its neighbors, which will for $t < 0.05$ ps perform harmonic vibrations and librations. On the other hand, on longer times the cage can relax, and the water molecule will diffuse and cooperatively form a new cage. This is the so-called RCM model

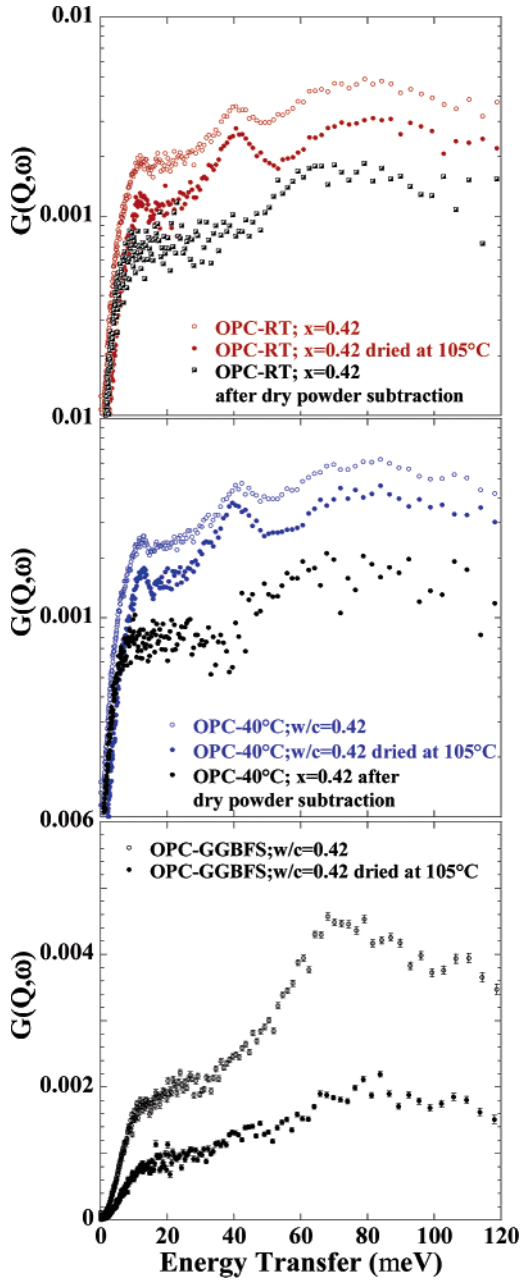

Figure 2. Density of states of the hydrogen atoms for the samples with w/c = 0.42 (NEAT, $\langle Q \rangle$ =1.18 Å^{-1}, ΔE = 98 μeV). The suppression of the water vibrations was also observed in other systems containing confined water.[23,60] For a better visualization of the OPC pastes the *y*-scale is logarithmic.

(random cage model) that was applied to calculate the generalized frequency distribution of the vibrational motions of supercooled water[21] as well as to reconstructed density of states for hydrated calcium silicate pastes.[22] Both experiments and MD simulations have shown the existence of two peaks in the GDOS centered at about 10 and 30 meV that are attributed to translational motion of the water molecules inside the cage.[21−23]

As seen in Figure 2 the spectra of the hydrated OPC samples are very similar with maxima around 10, 40, and 80 meV. However, in the case of the GGBFS paste, where the hydration process is expected to occur at a slower rate and the calcium hydroxide is expected to react with the GGBFS,[2] the peak around 40 meV that originates from vibrations[24−26] of the Ca(OH)$_2$ is not visible. Moreover, the inelastic spectra obtained after the dried powder subtraction for the OPC samples, also shown, can be assigned to water vibrations caused by the matrix confinement. Such spectra are similar to the spectra of water confined in Vycor, where it was shown that the strong peak observed at 6 meV, due to bending motions, is extremely attenuated.[23] Note that the accuracy of the data does not allow us to unambiguously determine if the shift to higher energy of the librational peak (observed in bulk water at about 70 meV) does in fact take place. Such shifts are related to reduction of the degrees of freedom and hindrance of the motions.[7] However, our experimental results correlate well with molecular dynamics calculations as described above in this section.

B. Quasielastic Response. (*i*) *From Picosecond to Nanosecond Dynamics of Protons.* It is important to keep in mind that before hydration, OPC consists of a mixture of four clinker phases which are interground with gypsum. Tricalcium silicate (Ca_3SiO_5) is the most abundant, followed by dicalcium silicate (β-Ca_2SiO_4), calcium aluminate ($Ca_3Al_2O_6$), and Browmillerite ($Ca_4Al_2Fe_2O_{10}$). After 28 days of reaction the tricalcium silicate is normally about 75% reacted while dicalcium silicate and the Browmillerite will not be as fully hydrated. At 28 days the paste is hard but further reaction can still take place.[2] As described in the Introduction, as cement paste sets the calcium silicates react with water to form the calcium silicate gel (defined as C−S−H) and calcium hydroxide that will be characterized by both their chemical composition and their structural and dynamical properties. Considering that a rather unique tool to gain experimental information on water dynamics in the picosecond range (from 0.1 to a few hundred picoseconds) is incoherent inelastic neutron scattering (IINS), which takes advantage of the large incoherent scattering cross-section of hydrogen atoms with respect to the relatively small cross-sections of other constitutive atoms in cement paste, the dynamics of hydration water in tricalcium silicate and dicalcium silicate has been carefully studied by means of QENS;[8,15,16,22,25,27,28] however, not much has been reported using the technique in hardened cement pastes with different levels of hydration. Nonetheless, by means of proton NMR measurements[29−31] three states of mobility have been identified in hardened cement pastes: (i) protons confined in solid phases such as hydroxyl groups chemically bound into the C−S−H structure; (ii) semiliquid-like water that can hydrogen bond (less strongly) to the C−S−H at the pore surface, defined as "glassy-water" due to its similar behavior to supercooled bulk water;[15] and (iii) and bulk-like pore water, the unbound molecules that are confined within the pores.

Furthermore, it was also observed that heating cement pastes at 105 °C results in the removal from the cement paste of both the glassy and the unbound water, so that only the chemically bound water remains in the sample.[29] As mentioned in the previous section, during our experiments no QE broadening was detected on the NEAT and HFBS spectra (see Figure 1) after the heating process. This observation indicates that the dynamics of chemically "bound" water molecules occurs on a time scale significantly slower than the nanosecond. This assumption is further supported by the earlier QENS studies of Hall et al.[32] on the dynamics of interlamellar water in clays. In their work it was showed that H bound to the clay is immobile on the time scale of the neutron measurements (10^{-10}−10^{-13} s), and that the QE signal is due entirely to the noncoordinated water. In addition, one can expect that the chemically bound water molecules dynamics is essentially of rotational origin. Moreover, Fratini et al.[15] have also demonstrated by means of QENS experiments on tricalcium silicate that using a good energy resolution (28 μeV) yields a clear identification of the "glassy-like" water and negligible contribution from the bulk water, and

that the chemically bound water is immobile on the times scales of their experiments. Their results in fact agree with the results from other QENS experiments performed by FitzGerald et al.[16,25] that have shown that on cement pastes hydrated for more than 28 days the unbound water molecules dynamics occurs on a time scale of the order of the picosecond. In FitzGerald[16,25] work the energy resolution was much more relaxed (146μeV), thus probing an extended time scale that allowed for the observation of the unbound water contribution.

Here in order to address the question about the states of water mobility in hardened cement pastes the neutron scattering studies were focused on the quasielastic (QE) region of the IINS spectrum to probe diffusive motions in a broad time scale (from a few nanoseconds to a few hundred picoseconds) that will be dominated by proton motion. Such protons will be involved not only in the water molecule rotation around their center of mass (scattering function denoted $R(Q,\omega)$), but also in long-range translational motions (scattering function denoted $T(Q,\omega)$), which occur on two different time scales.[33] In reality, ignoring contributions from rotations will tend to assign a broader width to the "translational" Lorentzian and result in a shorter mean residence time.[34] Assuming that the motions are noncorrelated results in the convolution of the scattering laws associated with the translational and rotational contributions as given below:[35]

$$S(Q,\omega) = -e^{\langle u^2\rangle Q^2}\{(1-C)[T(Q,\omega)\otimes R(Q,\omega)] + C\delta(\omega)\}\otimes F(Q,\omega) + B(Q) \quad (2)$$

The first term is the Debye−Waller factor where $\langle u^2\rangle$ denotes the mean square displacement of the proton. The term $B(Q)$ is a flat background. Both factors describe the inelastic contribution to the spectral intensity, which is expected to occur at energies large compared to those of the quasielastic region. C is the fractional elastic contribution coming from the water molecules that are bound to the cement paste, while the fraction of free hydrogen atoms ($1 - C$) is assumed to be water-like. $\delta(\omega)$ is the Dirac function. In practice the finite resolution of the instrument is also to be taken into account, so the observed $S(Q,\omega)$ is modeled by convoluting the theoretical scattering function to the experimental resolution function $F(Q,\omega)$.

For a classical rotational motion on the surface of a sphere, where a is the radius of gyration, $R(Q,\omega)$ is given by the Sears expansion:[36]

$$R(Q,\omega) = j_0^2(Qa)\delta(\omega) + \frac{1}{\pi}\sum_{l=1}^{\infty}(2l+1)j_l^2(Qa)\frac{l(l+1)D_r}{(l(l+1)D_r)^2+\omega^2} \quad (3)$$

The first term represents the elastic response of the system, whose energy dependence is accounted for by a Dirac delta function. The Q-dependence is provided by $j_0^2(Qa)$ that represents the elastic incoherent structure factor, hereafter denoted EISF. It is correlated to the number density of bound water. D_r is the rotational diffusion constant, characterized by a relaxation time $\tau_r = 1/6D_r$, and j_l are the spherical Bessel functions. In fact, by taking a radius of gyration as the O−H distance in a water molecule (0.98 Å), only the first four terms of the Sears expansion are significant in the present experimental Q-range.

The long-range translational component, $T(Q,\omega)$ is commonly modeled by a Lorentzian with half-width at half-maximum $\Gamma_T(Q)$,

$$T(Q,\omega) = \frac{1}{\pi}\frac{\Gamma_T(Q)}{\Gamma_T^2(Q)+\omega^2} \quad (4)$$

Considering a random diffusion process, the variation of Γ_T vs Q can be approximated by the model of Singwi and Sjölander:[35,37]

$$\Gamma_T(Q) = \frac{D_t Q^2}{1 + D_t Q^2\tau_0} \quad \text{and} \quad D_t = \frac{L^2}{6\tau_0} \quad (5)$$

where D_t is the self-diffusion coefficient, τ_0 is the average residence time between jumps, and L is the mean jump distance.

A typical quasielastic neutron scattering spectra obtained with NEAT for the cement paste with w/c = 0.42 with $\Delta E = 98$ μeV at selected Q values, together with the fitted curve obtained with the model described above, is illustrated in Figure 3. One can observe an excellent agreement between the fitted model and the experimental data. The behavior of the extracted half-width at half-maximum (Γ, hwhm), from the $\Delta E = 98$ μeV measurements, is represented in Figure 4.

The fitted parameters, characterizing the rotational and translational motions of unbound water as well as the fraction of bound water, are given in Table 2. The diffusion constants, D, and the residence time, τ_0, values obtained from the analysis of our QENS data are in broad agreement with observations of diffusion motion of water in other confined systems at room temperature.[38−40] In particular, we note that the translational diffusion of water in the hydrated cement paste is slower than that in pure water. Furthermore, the OPC-GGBFS pastes are known to hinder chloride diffusion and so the observed reduction in the water diffusion in this paste is not surprising. The increase of the mean residence time, τ_0, can be attributed to deviations of the structure from the ideal hydrogen-bonded network. Indeed as shown in Figure 5 the larger the mean jump distance (L), which reflects the local tetrahedral arrangement of the water molecule, the longer the residence time. On the other hand, the rotational correlation time τ_r is very similar to the rotational correlation time determined by QENS for single water molecules and for the one-H_2O layer Li-montmorillonite.[41]

Keeping in mind that the time scale at which the correlation functions are probed is determined by the energy resolution ΔE of the spectrometer, by employing various energy resolutions, different time domains and characteristic mobility are accessible. To reliably probe the slower translation attributable to the physically bound water, we used an incident neutron wavelength of 8.1 Å, with $\Delta E = 30$ μeV. Figure 6a shows an example of spectra obtained with NEAT in such a configuration for the cement paste with w/c = 0.42, namely OPC-40°C at selected $Q = 0.883$ Å^{-1}. The QE component was fitted with the model described above by eqs 2−5. Once again, because the data analysis was not confined to $Q < 1$ Å^{-1} the rotational contribution could not be neglected. In view of the fact that in this time scale one expects to monitor the physically bound, or "glassy", water, one has to take into consideration the hydration structure. In a first approach one can consider only the first hydration shell that consists of the first neighbor ion−water distances and the number of water molecules around the ion. Therefore during the fit procedure of the high-resolution ToF data the radius of gyration was also taken as a variable. The radius of gyration obtained in such a way, 2.5 Å, agrees very well with the Na^+−H_2O, Ca^{2+}−H_2O, and K^+−H_2O bond length obtained by diffraction methods and computer simulations.[42−44] Figure 6b shows the evolution of the hwhm as a function of

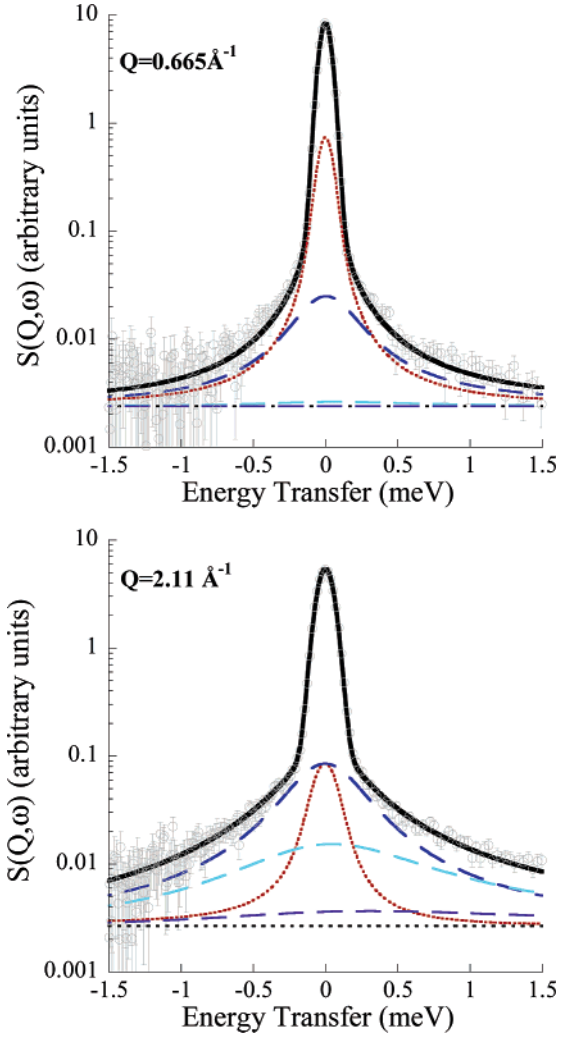

Figure 3. Examples of experimental spectra (○) at selected Q-values for the cement paste with w/c = 0.42, $\Delta E = 98$ μeV, together with the best fit (solid line) and the QE components (dotted lines represents the translational component and the long dashed lines represents the first three terms of the Sears expansion used to describe the rotational motion. The background is also shown (short dashed line). Notice how small the QE is (2% of the elastic signal).

Q^2. As expected, on this time scale the width of the QE component is much narrower, and shows a dependence in Q that reveals the existence of a second random diffusion process. A diffusion constant value of $D = (6 \pm 1) \times 10^{-10}$ m^2/s and an average residence time $\tau_0 = 51 \pm 3$ ps between jumps were obtained for the OPC-40°C with w/c = 0.42. These values are in broad agreement with observations of translational diffusion motion at room temperature of physically bound water.[11,32,45] Furthermore a relaxation time $\tau_r = 1/6D_r = 8$ ps agrees well with the rotational relaxation time obtained for interfacial water in dicalcium silicate with the RCM.[46] Therefore we can conclude that our QENS data provide evidence for the first time that in the picoseconds time scale two different random diffusion processes widely separated in time scale indeed occur in hardened cement pastes.

To analyze the HFBS data, and as discussed earlier,[47] an averaging procedure was needed to improve the statistical quality of the signal. In the first step of the analysis, the averaged spectra for a given water-to-cement ratio has been fitted by means of an elastic peak plus a Lorentzian function. As shown in Figure 7 such a model was inadequate, and an additional QE component (i.e., Lorentzian function) was added. The

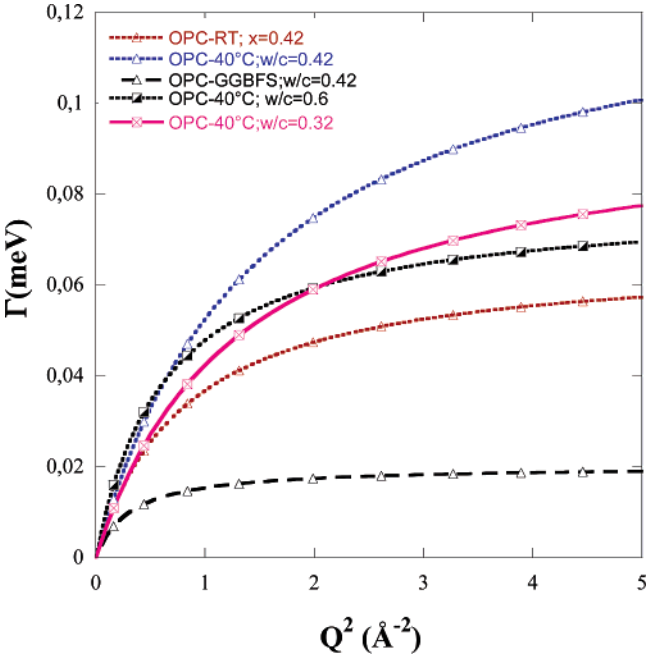

Figure 4. Line width (hwhm) as a function of Q^2 of the QE component for water contained in cement pastes, using 5.1 Å neutrons, with $\Delta E = 98$ μeV. The solid lines are fit to the data with the Gaussian jump-length distribution model. The obtained fit parameters are given in Table 2.

following phenomenological expression has been used to fit the experimental spectra:

$$S_m(Q,\omega) = F\{[A_0\delta(\omega) + A_1L_1(\Delta_1,\omega) + A_2L_2(\Delta_2,\omega)] \otimes F(\omega)\} + B \quad (6)$$

where F is a scaling factor, A_i are the structure factors, A_0 represents the EISF, $L_i(\Delta_i,\omega)$ are the Lorentzian functions having the half-widths at half-maxima (hwhm) Δ_i, and $F(\omega)$ is the experimental resolution function. The flat background term, B, represents the inelastic contribution and also includes the contribution coming from the unbound and physically bound water molecules observed by means of the NEAT experiments. Indeed, the QENS components associated with the unbound water are characterized by hwhm of the order of hundreds of millielectronvolts, thus too broad to be resolved by means of the HFBS experiments; the energy resolution is 1.1 μeV and, due to the backscattering geometry, the energy window is limited to ± 32 μeV.

As discussed in our earlier work,[47] the elastic contribution represents less than 0.1% of the total scattering and the backscattering spectra measured on HFBS probed two different motions (τ_0(ps) = $\hbar/\Gamma$(hwhm)), one slow motion of 6.6 ns characteristic time (corresponding to $\Delta_1 = 0.1 \pm 0.05$ μeV), and a faster one of 130 ps (corresponding to $\Delta_2 = 5 \pm 0.5$ μeV). The unbound water molecules contribution being considered within the flat background and the rotational dynamics of the chemically bound water molecules giving rise to a QENS component not resolved on the HFBS spectra, the slower motion might be associated with a long-range translational diffusion of the protons of the chemically and physically bound water molecules: there might be proton exchange between these two types of water molecules. However, in view of the averaging procedure of the spectra and considering the hwhm of this translational component ($\Delta_1 = 0.1 \pm 0.05$ μeV) with respect to the energy resolution ($\Delta E = 1.1$ μeV), it is difficult to unambiguously attribute this QENS component. The faster

TABLE 2: Parameters Characterizing the Rotational and Translational Motion of Water in Various Cement Pastes with w/c = 0.32, 0.42, and 0.6 at $T = 300$ K, $\Delta E = 98$ μeV[a]

sample	C	τ_r (ps)	L (Å)	τ_0 (ps)	D_t (10^{-9} m^2/s)
bulk water[34]		1.05	1.53	1.57 ± 0.12	2.49 ± 0.07
OPC-40°C; w/c = 0.32	0.91	1.6 ± 0.1	2.1 ± 0.2	6 ± 1	1.13 ± 0.08
OPC-RT; w/c = 0.42	0.88	1.63 ± 0.05	2.7 ± 0.3	10 ± 1	1.24 ± 0.01
OPC-40°C; w/c = 0.42	0.87	1.50 ± 0.08	2.0 ± 0.3	5.0 ± 0.6	1.33 ± 0.05
OPC-GGBFS w/c = 0.42	0.90	1.7 ± 0.07	4.36 ± 0.09	32 ± 6	1.0 ± 0.2
OPC-40°C; w/c = 0.6	0.77	1.61 ± 0.05	3.1 ± 0.2	8.4 ± 0.8	1.9 ± 0.1
OPC-40°C; w/c = 0.32	0.63	1.7 ± 0.1	1.42 ± 0.6	1.6 ± 0.1	2.09 ± 0.05
OPC-40°C; w/c = 0.6	0.5	1.15 ± 0.04	1.7 ± 0.6	2.04 ± 0.07	2.38 ± 0.06

[a] Values of bulk water are given for comparison. The values reported in the last two lines were obtained for the samples that were rehydrated after being dried at 105 °C in an oven to constant weight.

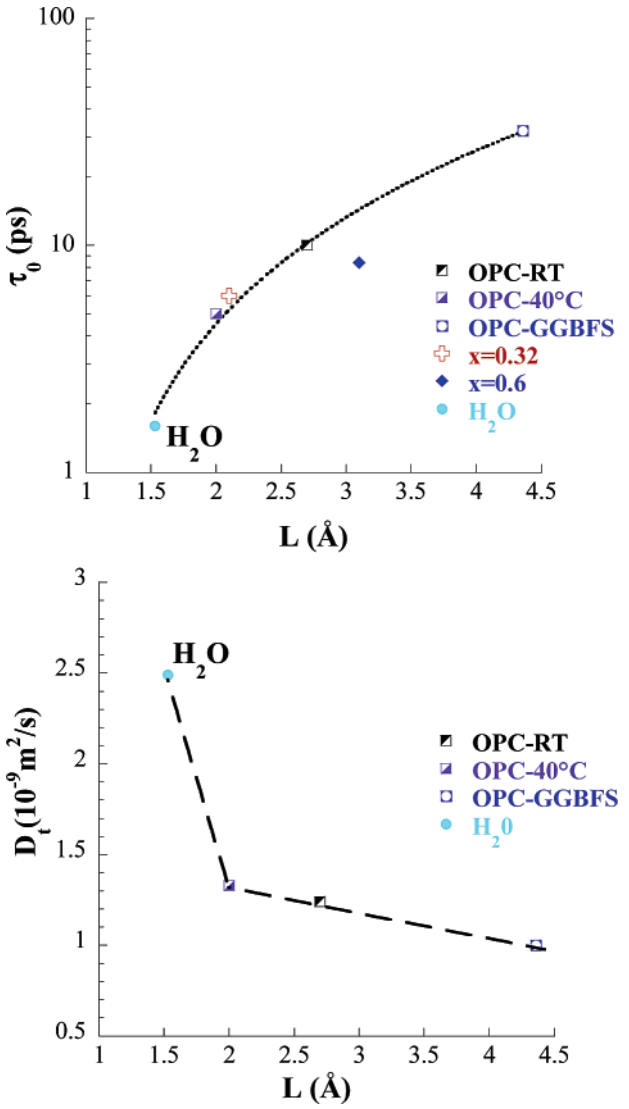

Figure 5. Dependences of the residence time (for the w/c = 0.42) and the average relaxation time of eq 5 on Q vs mean jump length. The straight lines are guides to the eye.

motion, which is 5 times slower than the one probed with NEAT, indicates the existence of another type of localized diffusive motion that can probably also be assigned to the physically bound water molecules. Following this assumption, the proportion of chemically and physically bound water molecules can be extracted from the structure factors A_1 and A_2. Their values for the sample prepared with w/c = 0.42 are ($A_1 = 0.89$, $A_2 = 0.11$) for OPC-RT and ($A_1 = 0.85$, $A_2 = 0.15$) for OPC-40°C.

(*ii*) *Percentages of Chemically Bound, Physically Bound, and Unbound Water in the Pastes.* At this point it is of interest to discuss the fractional elastic contribution (C factors given in Table 2). During the hydration process the chemically bound (or structural) water molecules will react with the paste and form a compound where the hydrogen is seem as immobile on the time scale of the NEAT or HFBS measurements, while the physically bound and unbound water are expected to give rise to the QENS signal on the ns and ps time scales, respectively. Given that the NEAT experiments were carried out on cement pastes hydrated for more than 28 days, one can consider that the elastic contribution comes from the chemically bound plus physically bound water molecules, with fractional contribution ranging from 77% to 91% as the water-to-cement ratio decreases. Moreover, for the same w/c ratio, we observe that the number of mobile water molecules was reduced in the OPC-GGBFS, while the value of still unbound water in the OPC-RT and OPC-40°C, 12% and 13%, respectively, agrees with the observation made in tricalcium silicate[25] with w/c = 0.4.

For the OPC-RT and OPC-40°C samples prepared with w/c = 0.42, using the structure factor values A_1 and A_2 determined by means of the HFBS experiment (given in the previous paragraph) and the fraction of unbound water determined by means of the NEAT experiment (C factors given in Table 2), the percentages of the three species of water molecules (chemically bound, physically bound, and unbound) can be determined and are given in Table 3. In this table, the percentages for cement after 2 days of hydration have also been reported.[27]

(*iii*) *Water Transport between the Gel and Capillary Pores.* When the cement is hydrated the free water will combine with the cement to form a paste with a developing pore structure. After 28 days most of the original water is locked into the hydration products that make up the cement paste and this water is the chemically bound water. Such water will not be found in the pores. This pore structure will continue to grow and develop slowly over long time perhaps even for decades. Some water will be found in the partially filled capillary pores and this water will mainly be in the "unbound state". The translational motion of the unbound water is slower by a factor of 2−3 (see Table 2), indicating that in fact as in 2D vermiculite clays at least some of the water behaves like bulk.[39] The gel pores, which are defined to be less than 100 Å in diameter, can be assumed to have the majority of the physically bound water. This assumption can be justified by the fact that these pores contain the majority of the surface area of the paste. The water in this confined space should mostly be physically bound to the calcium−silicate−hydrate gel. As demonstrated in Section B(i) the QENS spectra shows both rotation and translational diffusion motion but in a different time scale as the water in the "unbound state" found in the capillary pores. Both translational and

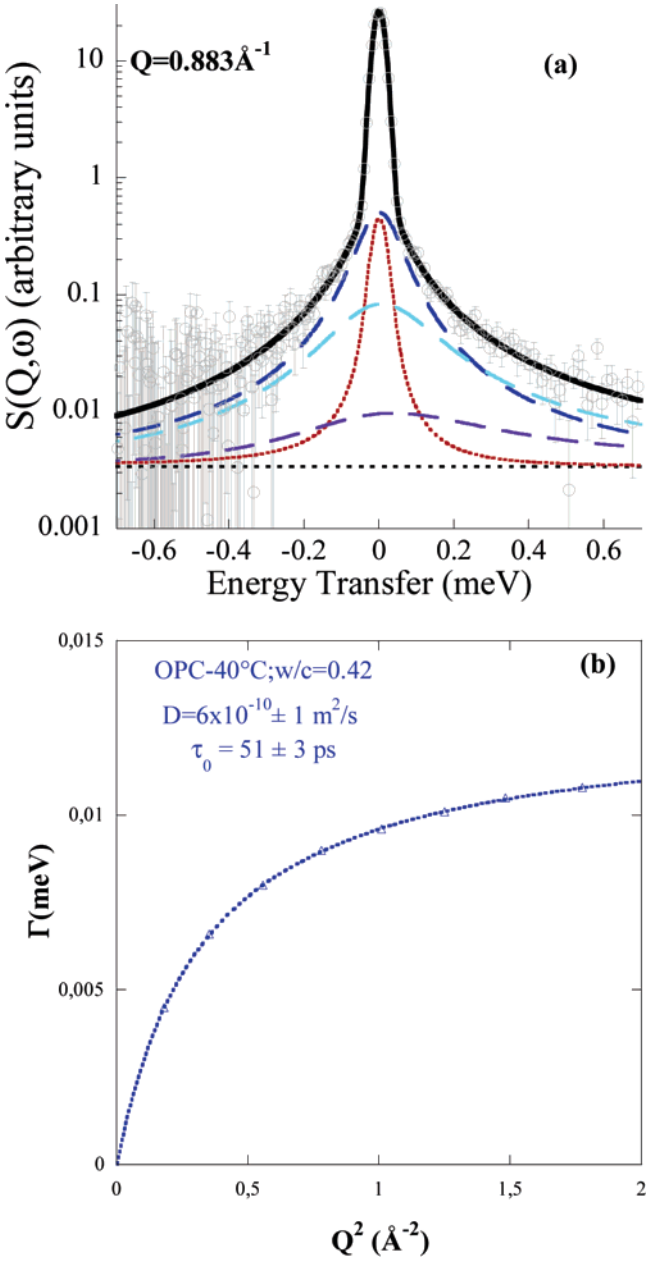

Figure 6. (a) Experimental spectrum (○) at $Q = 0.883$ Å^{-1} for the cement paste OPC-40 °C w/c = 0.42, $\Delta E = 30$ μeV, together with the best fit (solid line) and the QE components (dotted lines represent the translational component and the long dashed lines represent the first three terms of the Sears expansion used to describe the rotational motion. The background is also shown (short dashed line). Notice how small the QE is (2% of the elastic signal). (b) Line width (hwhm) of the translational Lorentzian $\Gamma_T(Q)$ of eq 5 as a function of Q^2 of the QE component for water contained in cement pastes, using 8.1 Å neutrons, with $\Delta E = 30$ μeV. The solid lines are fit to the data with the jump diffusion model, giving a diffusion constant value of $D = (6 \pm 1) \times 10^{-10}$ m^2/s, an average residence time $\tau_0 = 51 \pm 3$ ps, and a relaxation time $\tau_r = 1/6D_r = 8$ ps. Comparison of Figures 3, 4, and 6 provides clear evidence that in the picosecond time scale two different random diffusion processes widely separated in time scale occur in hardened cement pastes.

rotational motions are much slower than bulk water, and agree with the idea that confinement increases with curing time.[46]

It is the transfer of the water between the capillary and gel pores that dominates many important properties of concrete. The durability of concrete has been inversely associated with the ability of the concrete to transfer fluids[3] and as good concrete has discontinuous capillary pores the bottleneck for water

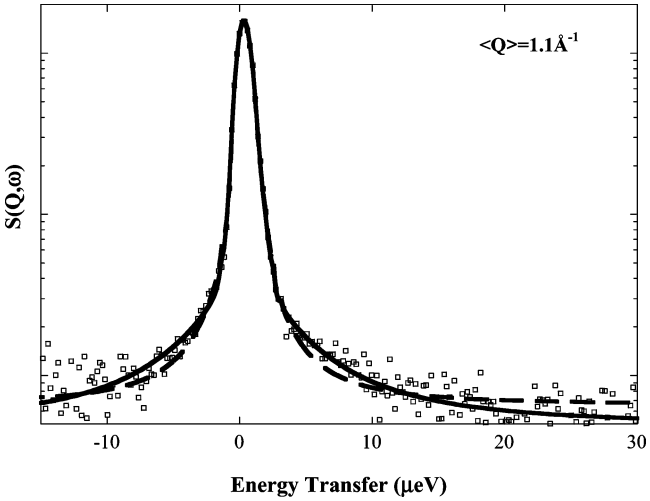

Figure 7. Experimental QENS spectrum ($\langle Q \rangle = 1.1$ Å^{-1}) recorded at w/c ratio 0.4 prepared at room temperature compared to the fitted curves for the two phenomenological models described in the text: one elastic peak plus one Lorentzian function (thin dashed line) and one peak plus two Lorentzian functions (continuous line).

TABLE 3: Percentages of Chemically Bound, Physically Bound, and Unbound Water in Cement Pastes with w/c = 0.4 After 2 (according to ref 27) and 28 days of Hydration (this work)

	OPC-RT with w/c = 0.4		OPC-40°C with w/c = 0.4	
	2 days[27]	28 days	2 days[27]	28 days
unbound water (%)	22.5	12	14.6	13
physically bound water (%)	17.4	10	19.7	13
chemically bound water (%)	60.1	78	65.7	74

transport will be the transfer of water in the gel pores.[5] Another important example is where concrete is used to condition and contain nuclear waste[48] and here the transfer of water through concrete will be governed by the transfer of water between the gel pores. It is also considered that water plays an important role in creep and shrinkage of concrete[2,3] and an understanding of the transfer of water in the gel pores could help in understanding these phenomena. It can be generally assumed that there is less water than there is pore volume. Water is easily removed from the pores of the paste by evaporation or is easily adsorbed into the pores depending on the relative humidity of the surrounding atmosphere. It is expected that the water will redistribute itself between the capillary and gel pores as the pore capacity is generally greater than the water present in the paste. Because of the attraction of water into the narrower gel pores it is generally assumed that water will be preferentially removed from the larger pores and that the extent of the removal will be dictated by known physical laws. It has been calculated that pores of diameter larger than 50 Å will be empty when the relative humidity is about 65%.[49]

As detailed in the Experimental Section, after the QENS spectra were recorded, the pastes were heated at 105 °C and the QENS spectra remeasured. Water was then added to these pastes over a 12 h period and the QENS spectra for the samples with a w/c ratio of 0.32 and 0.6 were remeasured. The spectra have been fitted by using the model given by expressions 2−5. As shown in Figure 8 the quality of this fit is good. As can be seen in Table 2, the rehydration water molecules behave as bulk water. This is a quite surprising result, and seems to indicate that there is a subtle interaction between the amorphous paste and the water, and removal of water seems to disturb the pore structure, which makes it difficult for the water to re-enter the

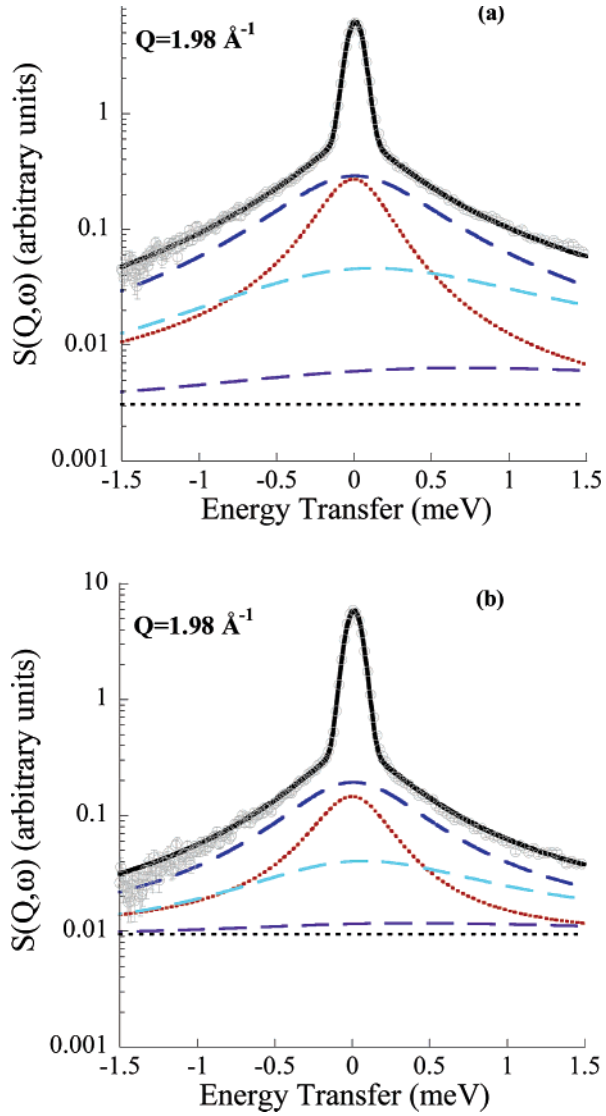

Figure 8. Examples of experimental spectra (○) at $Q = 1.98$ Å^{-1} for the cement paste with w/c = 0.32 (a) and 0.6 (b), $\Delta E = 98$ μeV, after the rehydration process explained in the text. The best fit (solid line) and the QE components (dotted lines represent the translational component and the long dashed lines represent the first three terms of the Sears expansion used to describe the rotational motion). The background is also shown (short dashed line).

gel pores. Such constrictions may be the key to understanding the transport of water in cement pastes.

The differences between the original water (with the three divisions unbound, physically bound, and chemically bound) and the rehydrated water with bulklike behavior are hard to explain. If a complete collapse of the gel pores occurs at 105 °C this would explain the differences. While some collapse will take place this scenario seems highly unlikely in view of the relatively high surface area of cement pastes dried at 105 °C.[4]

In reality gel pores in cement paste are not completely understood with many of the details controversial. Brunauer and co-workers[50,51] have measured the surface area of pastes made both from cement and calcium silicates and from water adsorption techniques. High surface areas of around 200 m^2/g were observed in cement pastes leading to the conclusion that much of the gel water was held in an interlayer similar to that found in clay. They suggested that the pores had narrow necks—what surface chemists call "ink bottle pores"—where constrictions in the necks of the pores presented an energy barrier, which inhibited the diffusion of water in to and out of the pore. It was then demonstrated that water was slowly removed and adsorbed equilibrium was not reached until the paste had been exposed to the water vapor for three months. Parrott et al.[52] observed that the drying of saturated tricalcium silicate pastes to a relative humidity in the range between 0.3 and 0.8 was a particularly slow process generally taking about 14 days.

It is tempting to speculate that the difference between the rehydration water and the original water is due to the slow passage of water into the gel pores and that the 12 h is too short a period for the water to be able to reoccupy the interlayer space. If such speculations are valid then we have a better understanding of water transport in the cement paste. It is imperative that these results are confirmed by careful experimentation of pastes stored at different relative humilities and after adsorption of water at well-chosen times. It is strongly suggested that such studies be carried out with both cement pastes and hydrated "pure cement" compounds such as tricalcium silicate. It is expected that pure tricalcium silicate will not contain the alkali atoms found in cement up to 1 M concentration and it may very well be that the role of alkali ions is critical in understanding the water transport between the gel and the capillary pores. In the interlayer space of the clay montmorillonite the amount of water allowed in the clay is critically dependent on the type and concentration of the cations present.[53] Thus the bonding in the interlayer space of the gel pores may be very similar to that described in clays as described by Malikova et al.[54,55] Indeed it should be noted that the diffusion of water in the interlayer water in clay is similar to that found here.[54,55] If these speculations are valid then the role of the ions in interlayer and gel pores must be understood.

Conclusions

In this paper we report for the first time a comprehensive analysis of the quasielastic response of water contained in concrete adding further information to the studies of nonequilibrium processes in complex formation reaction, contributing to the studies on dynamics processes of ions and water molecules.[56]

To address the question of water mobility in hardened cement pastes our studies focused on the QE response of the IINS spectrum. It is widely accepted that during the hydration process the free water will become either bound into the C−S−H gellike structure or will chemically react to form calcium hydroxide. Considering that by heating the samples at 105 °C no QE signal was detected in the whole time scale probed in these experiments we assume that both the physically bound and the unbound water were removed, while the chemically bound water remained. Thus the QE signal observed can be explained as local diffusive motions due to chemical/physical confinement, originating from the bulk water that reacts with the cement, plus geometrical confinement, caused by restricted volume. Similar water dynamics was reported in tricalcium silicate, a major component of OPC, by Fratini et al.[15] In their work QE experiments were performed with use of a energy resolution $\Delta E = 28$ μeV covering a Q-range from 0.55 to 1.24 Å^{-1} where the rotational motion could be neglected. Their spectra were analyzed with a dynamical model that indeed considers the existence of two water types which correspond to our chemically bound water and constrained-unbound water.

In complex systems such as the hardened cement pastes, it is not easy or straightforward to determine the origin of the observed differences in the dynamical behavior of the water molecules. However, by performing a series of QENS experi-

ments on a broad time scale we were able to gather important information on the water transport on hardened cement pastes with a w/c ratio varying between 0.32 and 0.6. The diffusion properties obtained from our data indicate that at least two diffusion processes occur, a fast diffusion likely attributable to unbound water confined in the pore structure ($D \approx 10^{-9}$ m^2/s) and a slower diffusion due to gel pore water ($D \approx 10^{-10}$ m^2/s). In addition from the high-resolution backscattering measurements a slowest motion was also detected, most likely associated with a long-range translational diffusion of the protons of the chemically and physically bound water molecules: there might be proton exchange between these two types of water molecules. This work indeed confirms the interpretation of previous NMR experiments, where three different types of water molecules were observed,[29−31] chemically bound water, physically bound water, and confined water, in hardened Portland cements.

Furthermore, this study has indicated the existence of differences in water diffusion of the glassy water in pastes (made with the same w/c ratio) but cured at different temperatures. This diffusion of water is significantly less in pastes made when OPC is replaced with GGBFS. It is not straightforward to explain this behavior, which is now under further investigation. Moreover, it has not escaped our attention that the water diffusion detected in our QENS measurements is similar to that described in the interlayer water of clays. It is certainly tempting to speculate that the role of ions in the bonding of the glassy water is similar to that described by Malikova et al.[54,55] For this reason the bonding of cations in clays and pastes with glassy water is also the subject of further investigation. In addition it is worth mentioning that the question of how long water molecules stay in the hydration shell is interesting, but rather complex. Molecular dynamics simulations may help answer this question and it is noteworthy that the residence time of the water molecules in the various cement pastes investigated in this work is comparable with the residence times of water molecules in the first hydration shell for Na^+ as determined by molecular dynamics simulations.[57]

It is also important to refer to very recent measurements where the diffusion of water in cement paste by NMR shows a similar magnitude to those found in this work,[58] and these results are significantly smaller, by about 2 orders of magnitude, than the bulk diffusion coefficients estimated from the diffusion of tritiated water.[59] The difference between the effective and the bulk diffusivity is often explained by the so-called tortuosity factor, which is related to the confining effect of walls on the diffusion of water. Considering that the QENS results reported here do reflect the diffusion of the water in gel pores then this suggests that the transport of water through cement paste is not significantly hindered by the transport through the gel pores but by another agency perhaps due to transport through the interfaces between the gel and capillary pores.

To conclude it was shown that the intensity in the first mode of the GDOS is reduced indicating a limitation on the water motion. From the comparison of the proton weighted density of vibrational states of water in cement pastes compared to pure water we could clearly observe the reduction of the intensity of the first mode, centered at 6 meV and assigned to transverse (bending) motions of the whole water molecule. As in other confined systems this observation indicates a limitation on the motion of water. Similar behavior is observed for the proton weighted density of vibrational states of water in Vycor and the water/DMSO mixture and water.[23,60]

There is still much to be learned in understanding the process of diffusion of water through concrete. First the procedures used in measurement and estimation of bulk diffusion using tritiated water may be flawed and procedures such as those outlined in refs 61−63 should be evaluated to see if they are needed. Second the effect of additives such as ground granulated blast furnace slag and fly ash on the gel pores of the calcium silicate hydrate gel should be determined to understand their contribution to the significant reduction of water diffusion. Third the role of cations in clay and cements during water entrance and exit from the interlayer should be evaluated. Last studies should be carried out separating the different components of water diffusion in cement (i) in the capillary pores, (ii) in the gel pores, (iii) in the interlayer, and (iv) between these regions. Both NMR and QENS methods should be used in these studies.

Finally, it is important to consider that although the models used here can only be a crude approximation of a much more complex dynamical behavior that takes place in hardened cement pastes, using these models a qualitative comparison of the different samples could be performed. As a consequence there appears to be no justification in fitting more complex models directly to the data.

Acknowledgment. The authors thank Z. Chowdhuri for her assistance during the HFBS measurements. We also acknowledge the support of the Berlin Neutron Scattering Center (BENSC) and of the National Institute of Standards and Technology, U.S. Department of Commerce, in providing the neutron research facilities used in this work. H.N.B. thanks R. E. Lechner for fruitful discussions. L.P.A. thanks the support from the Australian Access to Major Research Facilities Program.

References and Notes

(1) Sakamoto M.; Brockhouse B. N.; Johnson R. G.; Pope N. K. *J. Phys. Soc. Jpn.* **1962**, *17*(Suppl. B II), 370.
(2) Mindess, S.; Young, J. F.; Darwin, D. In *Concrete*, 2nd ed.; Prentice Hall: Upper Saddle River, NJ, 2003.
(3) Neville A. M. In *Properties of Concrete*, 4th ed.; Prentice Hall: Upper Saddle River, NJ, 1995.
(4) Garci Juenger, M. C.; Jennings, H. M. *Cem. Concr. Res.* **2001**, *31*, 883.
(5) Powers, T. C.; Copeland, L. I.; Mann, H. M. *J. PCA Res. Dev. Lab. L* **1959**, 38.
(6) Poinsignon, C.; Estrade-Szwarckopf, H.; Conard, J.; Dianoux, J. *Phys. B* **1989**, *156* & *157*, 140.
(7) Chen, S.-H.; Bellisent-Funel, M.-C. In *Hydrogen Bond Network*; Kluwer Academic Publishers: Amsterdam, The Netherlands, 1994; pp 307−336.
(8) Berliner, R.; Popovici, M.; Herwig, K. W.; Berliner, M.; Jennings, H. M.; Thomas, J. J. *Cem. Concr. Res.* **1998**, *28*, 231.
(9) Bordallo, H. N.; Herwig, K. W.; Dozier; W. D.; Drake, F. *J. Phys. IV* **2000**, *10*, 207.
(10) Mamontov, E. *J. Phys. Chem.* **2004**, *121*, 9087.
(11) Crupi, V.; Majolino, D.; Venuti, V. *J. Phys.*: *Condens. Matter* **2004**, *16*, S5297.
(12) Lechner, R. E. *Phys. B* **1992**, *180−181*, 973.
(13) Carpenter, J. M.; Pelizarri, C. A. *Phys. Rev. B* **1975**, *12*, 2391.
(14) Meyer, A.; Dimeo, R. M.; Gehring, P. M.; Neumann, D. A. *Rev. Sci. Instrum.* **2003**, *74*, 2759.
(15) Fratini, E.; Chen, S.-H.; Baglioni, P.; Bellisent-Funel, M.-C. *J. Phys. Chem. B* **2002**, *106*, 158.
(16) FitzGerald, S. A.; Neumann, D. A.; Rush, J. J.; Bentz, D. P.; Livingston, R. A. *Chem. Mater.* **1998**, *10*, 397.
(17) Cho, M.; Fleming, G. R.; Saito, S.; Ohmine, I.; Stratt, R. M. *J. Chem. Phys.* **1994**, *100*, 6672.
(18) Bellissent-Funel, M.-C.; Teixeira, J. *J. Mol. Struct.* **1991**, *250*, 213.
(19) Krishnamurthy, S.; Bansil, R.; Wiafe-Akenten, J. *J. Chem. Phys.* **1983**, *79*, 5863−5870.
(20) Chen, S.-H.; Gallo, P.; Bellissent Funel, M.-C. *Can. J. Phys.* **1995**, *73*, 703.
(21) Chen, S. H.; Liao, C.; Sciortino, F.; Gallo, P.; Tartaglia, P. *Phys. Rev. E* **1999**, *59*, 6708.
(22) Faraone, A.; Fratini, E.; Baglioni, P.; Chen, S.-H. *J. Chem. Phys.* **2004**, *121*, 3212.

(23) Bellisent-Funel, M.-C.; Chen, S.-H.; Zanotti, J.-M. *Phys. Rev. E* **1995**, *51*, 4558.
(24) Baddour-Hadjean, R.; Fillaux, F.; Floquet, N.; Belushkin, S.; Natkaniec, I.; Desgranges, L.; Grebille, D. *Chem. Phys.* **1995**, *197*, 81.
(25) FitzGerald, S. A.; Neumann, D. A.; Rush, J. J.; Kirkpatrick, R. J.; Cong, X.; Livingston, R. A. *J. Mater. Res.* **1999**, *14*, 1160.
(26) Thomas, J. J.; Chen, J. J.; Jennings, H. M.; Neumann, D. A. *Chem. Mater.* **2003**, *15*, 3817.
(27) Thomas, J. J.; FitzGerald, S. A.; Neumann, D. A.; Livingston, R. A. *J. Am. Ceram. Soc.* **2001**, *84*, 1811.
(28) Fratini, E.; Chen, S.-H.; Baglioni, P.; Cook, J. C.; Copley, J. R. D. *Phys. Rev. E* **1998**, *65*, 10201.
(29) Wang, P. S.; Ferguson, M. M.; Eng, G.; Bentz, D. P.; Ferraris, C. F.; Clifton, J. R. P. S. *J. Mater. Science* **1998**, *33*, 3065.
(30) Rakiewicz, E. F.; Benesi, A. J.; Grutzeck, M. W.; Kwan, S. *J. Am. Chem. Soc.* **1998**, *120*, 6415.
(31) Greener, J.; Peemoeller, H.; Choi, C.; Holly, R.; Reardon, E. J.; Hansson, C. M.; Pintar, M. M. *J. Am. Ceram. Soc.* **2000**, *83*, 623.
(32) Hall, P. L.; Ross, D. K.; Tuck, J. J.; Hayes, M. H. B. *Proc. IAEA Symp. Neutron Inelastic Scattering* (Vienna, 1977); International Atomic Energy Agency: Vienna, 1977; Vol. 1, pp 617−635.
(33) Teixeira, J.; Bellisent-Funel, M.-C.; Chen, S.-H.; Dianoux, A. J. *Phys. Rev. A* **1985**, *31*, 1913.
(34) Bordallo, H. N.; Herwig, K. W.; Luther, B. M.; N. E. Levinger, J. *Chem. Phys.* **2004**, *121*, 12457.
(35) Beé, M. In *Quasi-Elastic Neutron Scattering*; Adam Hilger: Bristol, Philadelphia, 1988.
(36) Sears, V. F. *Can. J. Phys.* **1966**, *44*, 1299.
(37) Singwi, K. S.; Sjölander, A. *Phys. Rev.* **1960**, *119*, 863.
(38) Tuck, J. J.; Hall, P. L.; Hayes, M. H. B.; Ross, D. K.; Poinsignon, C. *J. Chem. Soc., Faraday Trans.* **1984**, *80*, 309.
(39) Swenson, J.; Bergman, R.; Howells, W. S. *J. Chem. Phys.* **2000**, *113*, 2873.
(40) Nair, S.; Chowdhuri, Z.; Peral, I.; Neumann, D.; Dickinson, L. C.; Tompsett, G.; Jeong, H.-K.; Tsapatsis, M. *Phys. Rev. B* **2005**, *71*, 104301.
(41) Cebula, D. J.; Thomas, R. K.; White, J. W. *Clays Clays Miner.* **1981**, *29*, 241.
(42) Caminiti, R.; Licheri, G.; Paschina, G.; Piccaluga, G.; Pinna, G. *J. Chem. Phys.* **1980**, *72*, 4522.
(43) Einspahr, H.; Bugg, C. E. *Acta Crystallogr.* **1980**, *B36*, 264.
(44) Neilson, G. W.; Skipper, N. *Chem. Phys. Lett.* **1985**, *114*, 35.
(45) Faraone, A.; Liu, L.; Mou, C.-Y.; Shih, P.-C.; Brown, C.; Copley, J. R. D.; Dimeo, R. M.; Chen, S.-H. *Eur. Phys. J. E* **2003**, *12* , 15.
(46) Faraone, A.; Chen, S.-H.; Fratini, E.; Bablioni, P.; Liu, L.; Brown, C. *Phys. Rev. E* **2002**, *65*, 40501.
(47) Aldridge, L. P.; Bordallo, H. N.; Desmedt, A. *Phys. B* **2004**, *350*, e565.
(48) *Performance of engineered barrier materials in near surface disposal facilities for radioactive waste*; International Atomic Energy Agency; IAEA-TECDOC-1255 Vienna, IAEA, 2001.
(49) Powers, T. C.; Brownyard T. L. Studies of the physical properties of hardened Portland cement paste. In *Bulletin 22, Research Laboratories of the Portland Cement Association*; Portland Cement Association: Chicago, IL, 1948.
(50) Brunauer, S.; Odler, I.; Yudenfreund, M *Highway Res. Rec.* **1970**, *328*, 89.
(51) Hagymassy, J. J.; Odler, I.; Yudenfreund, M.; Skalny, J.; Brunauer, S. *J. Colloid Interface Sci.* **1972**, *38*, 20.
(52) Parrott, L. J.; Hanson, W.; Berger, R. L. *Cem. Concr. Res.* **1980**, *10*, 647.
(53) Norrish, K. *Nature* **1954**, *173*, 255.
(54) Malikova, N.; Marry, V.; Dufrêche, J.-F.; Simon, C.; Turq, P.; Giffaut, E. *Mol. Phys.* **2004**, *102*, 1965.
(55) Malikova, N.; Cadene, A.; Dubois, E.; Turq, P. *J. Phys. Chem. B* **2006**, *110*, 3206.
(56) Ohtaki, H.; Radnal, T. *Chem. Rev.* **1993**, *93*, 1157.
(57) Impey, R.W; Madden, P. A.; McDonald, I. R. *J. Phys. Chem.* **1983**, *87*, 5071.
(58) Nestle, N.; Galvosas, P.; Karger, J. *Cem. Concr. Res* In press.
(59) Atabek, R.; Bouniol, P.; Vitorge, P.; Bescop, P. L.; Hoorelbeke, J. M. *Cem. Concr. Res* **1992**, *22*, 419−429.
(60) Cabral, J. T.; Luzar, A.; Teixeira, J.; Bellissent-Funel, M.-C. *J. Chem. Phys.* **2000**, *113*, 8736.
(61) Atkinson, A.; Nickerson, A. K. *Nucl. Technol.* **1988**, *81*, 100.
(62) Bertram, W. K.; Rougeron, P.; Aldridge, L. P. *J. Aust. Ceram. Soc.* **1999**, *35*, 73.
(63) Tits, J.; Jakob, A.; Wieland, E.; Spieler, P. *J. Contam. Hydrol.* **2003**, *61*, 45.